Supporting Information

Lee et al. 10.1073/pnas.1303669110

SI Materials and Methods

Apoptosis PCR Array. The human Apoptosis PCR Array (SABiosciences, catalog no. PAHS-012) was used as described in the manufacturer's protocol. Data analysis was performed using the manufacturer's software package.

Mitochondria Isolation. Mitochondria and cytosol fractions were separated according to the instructions included with the Qproteome Mitochondria Isolation Kit (Qiagen, catalog no. 37612).

Real-Time PCR. RNA extraction and cDNA synthesis were performed as described previously (63). Gene-specific primers were as follows: hOCT4 (5-GCAGCTCAGCCTTAAGAACA-3, 5-GGCACTTCAGAAACATGGTC-3); hBIRC5 (5-GGACCACCGCATCTCTACAT-3, 5-GCACTTTCTTCGCAGTTTCC-3); hBCL10 (5′- TCCTCTCCTTCTTCCCCATT-3′, 5′-GGCGTCCTTCTTCACTTCAG-3′); β-actin (5-GTCCTCTCCCAAGTCCACAC-3, 5-GGGAGACCAAAAGCCTTCAT-3); α-SMA (5-AGAACATGGCATCATCACCA-3, 5-TACATGGCTGGGACATTGAA-3); hAFP (5-AGCTTGGTGGTGGATGAAAC-3, 5-TCTGCAATGACAGCCTCAAG-3); hBrachyury T (5-ACCCAGTTCATAGCGGTGAC-3, 5-CCATTGGGAGTACCCAGGTT-3); and hPAX6 (5-TGTCCAACGGATGTGTGAGT-3, 5-TTTCCCAAGCAAAGATGGAC-3).

Caspase-3 Activity Assay. The Ac-DEVD-AMC Caspase-3 Fluorogenic Substrate (BD Pharmingen) was used for assays performed according to the manufacturer's instructions.

FACS Analysis. For all of the FACS analysis, FACScalibur (BD Biosciences) and CellQuest software were used. Cells were stained using the PE Annexin V Apoptosis Detection Kit I (BD Pharmingen), FITC Rat Anti-SSEA-3 (BD Biosciences, catalog no. 560881), PE-Active Caspase-3 Apoptosis Kit (BD Biosciences, catalog no. 550914), and 7-aad (BD Biosciences, catalog no.559925) according to the manufacturer's instructions.

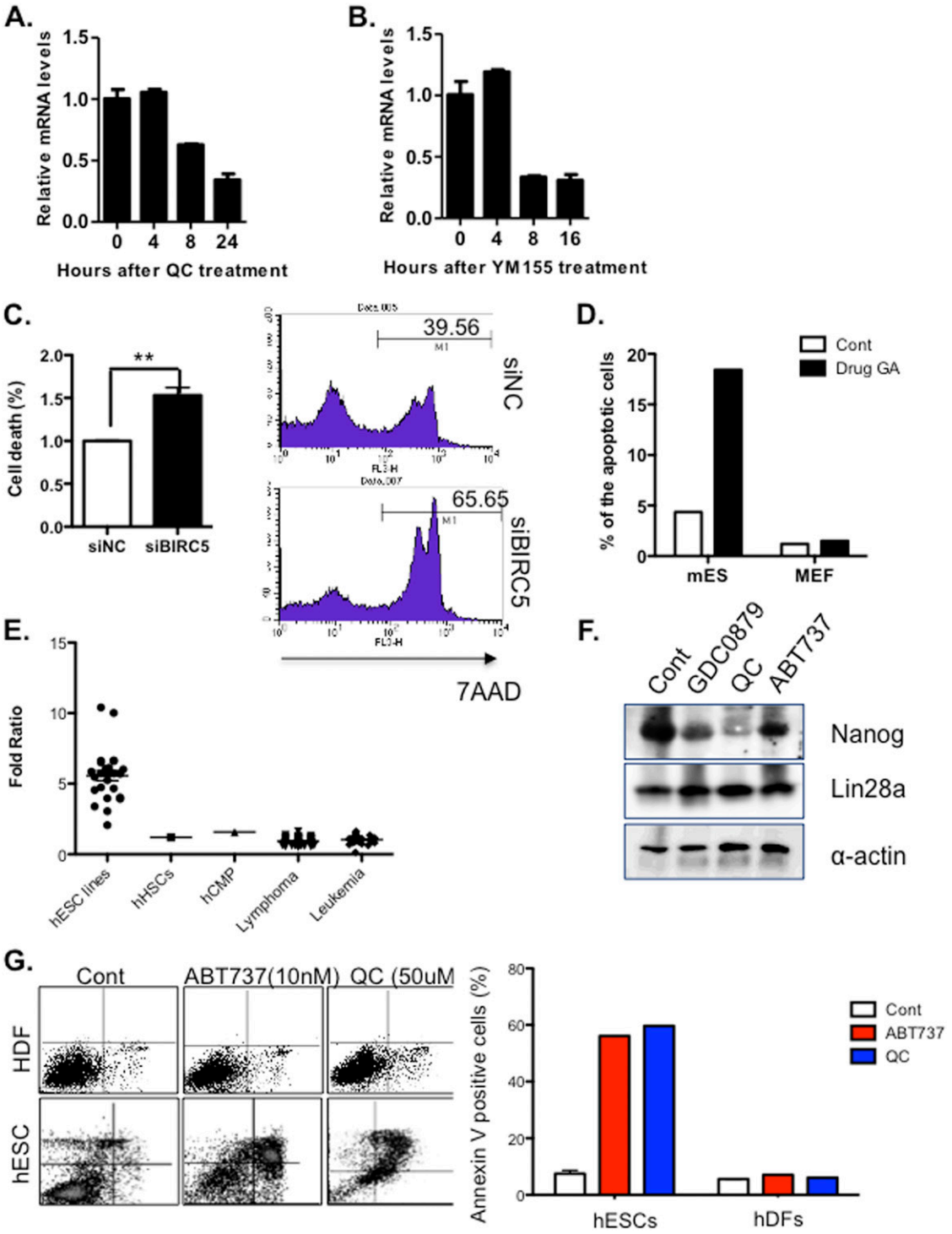

Fig. S1. hESCs were treated with 50 μM of QC (*A*) or 10 nM of YM155 (*B*) and were harvested at the indicated time. *BIRC5* expression level was determined by real-time PCR analysis. (*C*) *BIRC5* in hESCs was suppressed by 50 nM of siControl (siNC) or siBIRC5 using Dharmafect transfection reagent (catalog no. T-2001-01). Cell death rate was determined by FACS analysis stained with 7-aminoactinomycin D (7-AAD). FACS histogram (*Right*, with % of 7-ADD–positive population) and graphical image of cell death rates (*Left*). $^{**}P < 0.01$. (*D*) mESCs (J1 cells) or mouse embryonic fibroblasts (MEFs) were treated with 50 μM of gambogic acid (GA) for 24 h. Apoptotic population was determined by annexin V FACS analysis. Annexin V-positive population was graphically presented. (*E*) Expression level of *BIRC5* in hESC lines was compared with human hematopoietic stem cell (hHSCs), human common myeloid progenitor (hCMP), 70 lymphoma cell lines, and 33 leukemia cell lines revealed by a database search (www.nextbio.com), and relative expression level was presented in the mean value of a scatter plot. (*F*) hESCs were treated with 10 μM of GDC0879, 10 μM of ABT737, and 100 μM of QC for 24 h. Level of pluripotent markers, Nanog, and Lin28 was determined by immunoblotting analysis. Alpha-actin for loading control. (*G*) Flow cytometry plots of annexin V and 7-AAD staining after treatment with 10 μM ABT737 and 50 μM QC. Annexin V-positive cells were represented by bar graph.

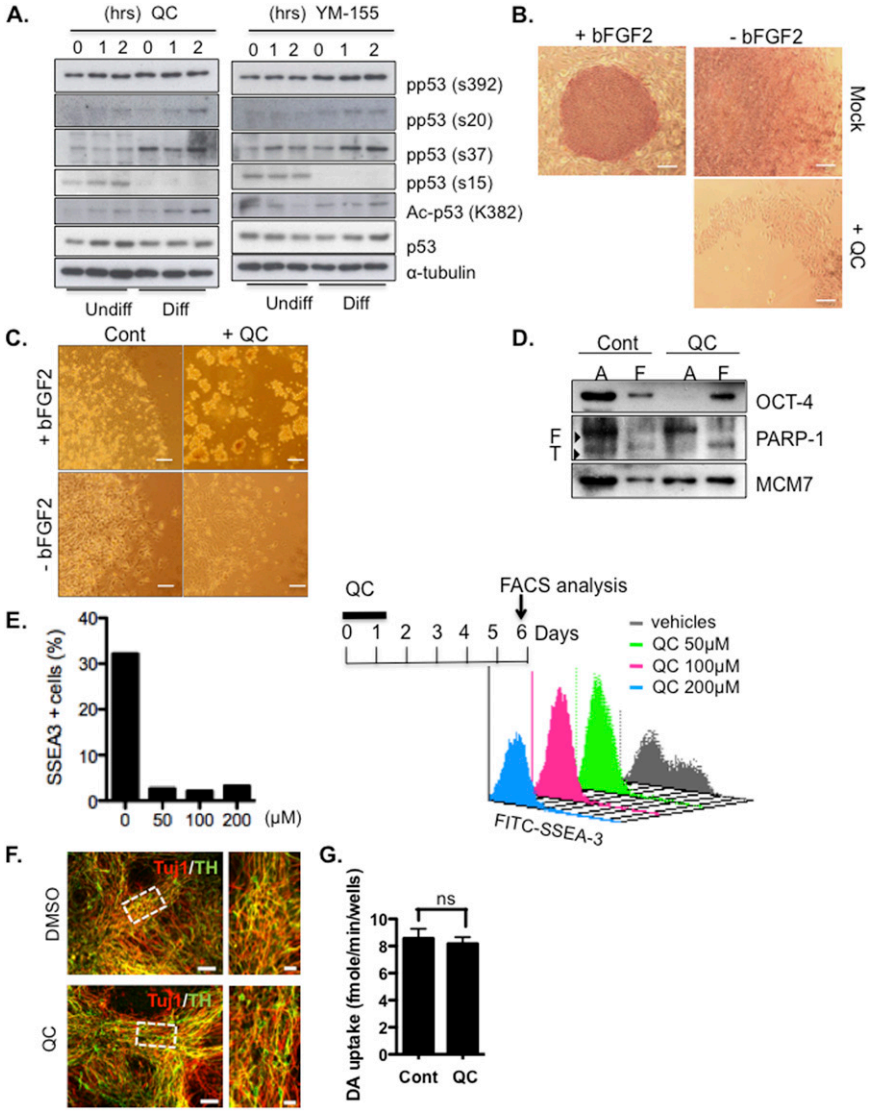

Fig. S2. (*A*) Human embryonic stem cells (hESCs) (Unidff) and spontaneous differentiated cells from embryoid bodies (EBs) of hESCs (Diff) were treated with either 50 μM of quercetin (QC) (*Left*) or 10 nM of YM155 (*Right*) for 24 h, and then protein lysates were subjected to the immunoblotting for indicative p53 posttranslational modification (PTM) antibodies. Alpha-tubulin for equal loading control. (*B*) Alkaline phosphatase staining of hESCs cultured in the presence or absence of bFGF2 (6 d) with or without 50 μM QC treatment for 24 h. (Scale bars, 200 μm.) (*C*) Light microscopic image of hESCs cultured with (*Left*) or without (*Right*) bFGF2 for 6 d, treated with 50 μM QC for 24 h. (Scale bars, 200 μm.) (*D*) Differentiated cells were treated with QC and then separately harvested with adherent and floating cells. Levels of OCT4 in adherent (A) or floating (F) hESCs before and after QC treatment were determined by immunoblotting. Poly (ADP ribose) polymerase-1 (PARP-1) cleavage (F, full length; T, truncated) was used as a marker of apoptosis, and minichromosome maintenance complex component 7 (MMC7) was used to verify equal loading. (*E*) FACS analysis of stage-specific embryonic antigen-3 (SSEA-3)–positive cells in mixed cell population after an additional 5 d with a single treatment with the indicated dose of YM155 (24 h). The resulting SSEA-3–positive population is represented as a graph (*Right*). (*F*) Dopaminergic neuronal cells derived from hESCs were treated with 50 μM of QC or vehicle for 24 h and were then subjected to dual immunostaining with Tuj (red) and tyrosine hydroxylase (TH) (green). (*G*) Dopamine uptake of dopaminergic neuronal cells treated with QC or vehicle (DMSO) for 24 h was determined by measuring incorporation of [^{3}H]-labeled dopamine using liquid scintillation. ns, not significant.

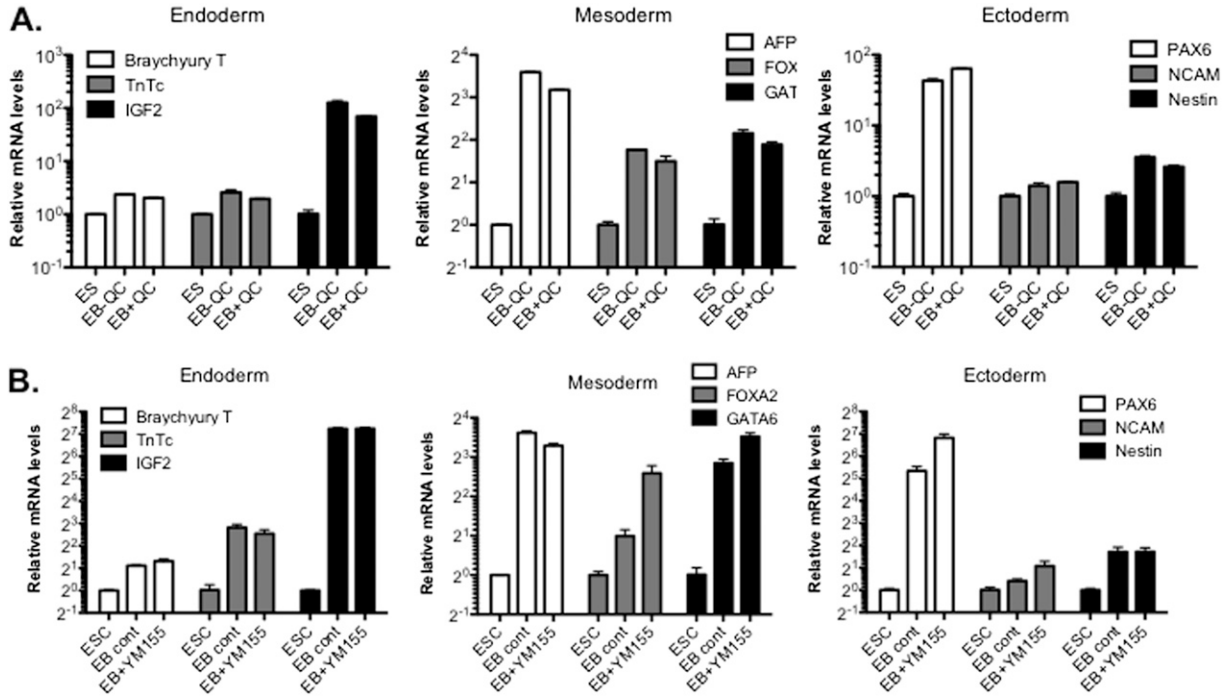

Fig. S3. Relative expression levels of lineage-specific differentiation markers (*AFP*, *FOXA2*, *GATA6* for endoderm; *Brachyury T*, *TnTc*, *IGF2* for mesoderm; and *PAX6*, *NCAM*, *Nestin* for ectoderm) of spontaneously differentiated hESCs in the presence (QC or YM155) or absence (NT) of 50 μM QC (*A*) or 10 nM of YM155 (*B*) for 24 h, compared with undifferentiated hESCs, were analyzed by real-time PCR analysis.

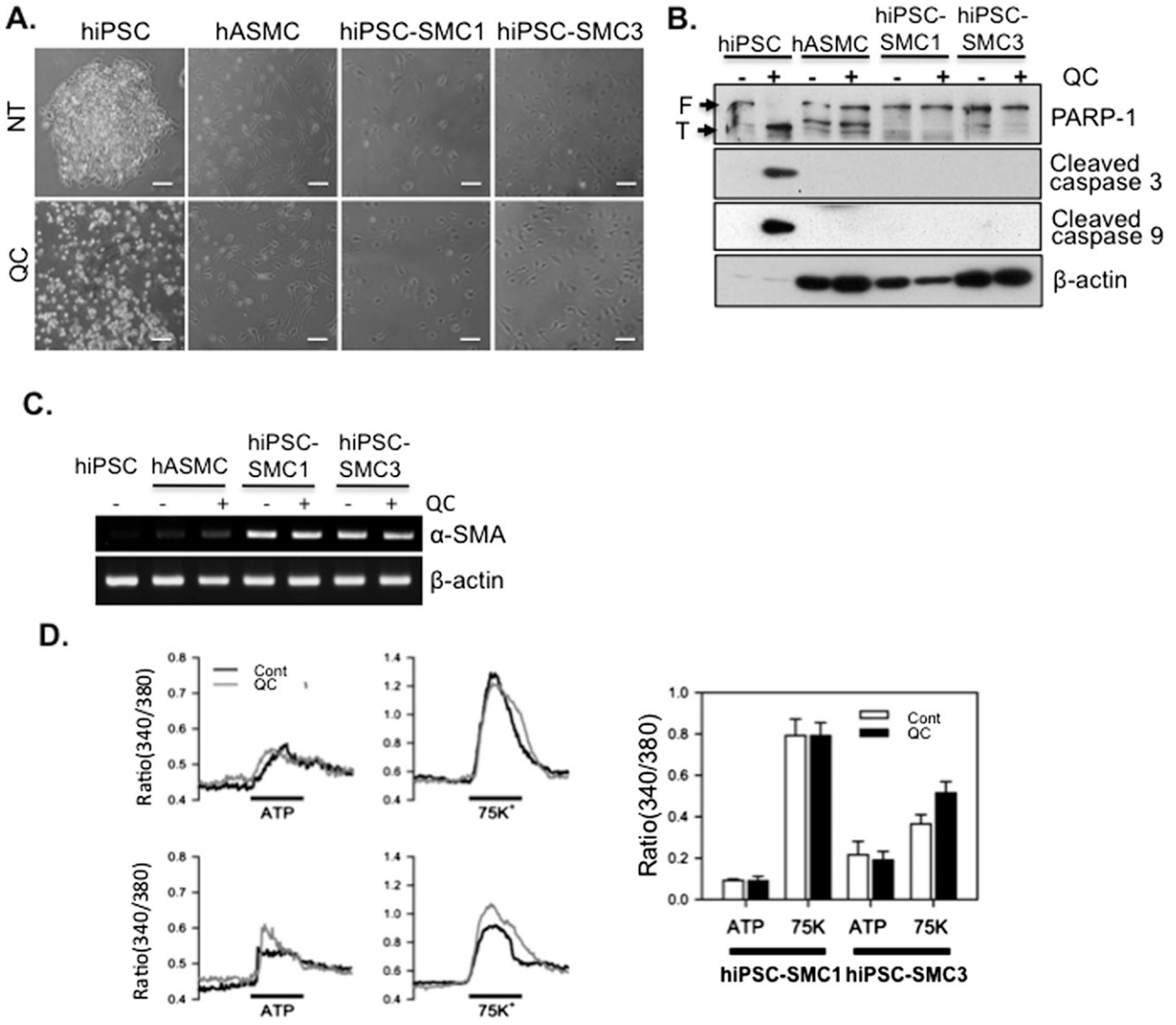

Fig. S4. Undifferentiated induced pluripotent stem cells (iPSCs) selectively undergo cell death in response to QC, whereas their differentiated counterparts are unaffected. (*A*) Light microscopic images of undifferentiated iPSCs, human aortic vascular smooth-muscle cells (hASMCs), iPSC SMC1 (hiPSC-SMC1), and hiPSC-derived SMC3 (hiPSC-SMC3) incubated in the presence or absence of 50 μM QC for 16 h. (Scale bars, 200 μm.) (*B*) Levels of PARP-1 cleavage (F, full length; T, truncated), cleaved caspase-3, and cleaved caspase-9 were determined by immunoblotting. Beta-actin was used as loading control. (*C*) The level of α-SMA mRNA was determined by RT-PCR. Beta-actin was used as loading control. (*D*) Relative change in intracellular calcium levels in response to a pharmacological agonist, ATP (20 mM; *Left*) or membrane depolarization (75 mM K^+; *Right*) in hiPSC-SMC1 (*Upper*) and hiPSC-SMC3 (*Right*) cells. The calcium response was tested before (black line) and after (gray line) treatment with 50 mM QC for 6 h, as described in *Materials and Methods*. Treatment with ATP or 75 mM K^+ is indicated by the black bar at the bottom of each panel. Net changes in intracellular calcium after treatment with ATP (white) or 75 mM K^+ (black). Changes in calcium level were expressed as the ratio (340/380) of Fura-2 emissions. Means + SEM; n = 18–23.

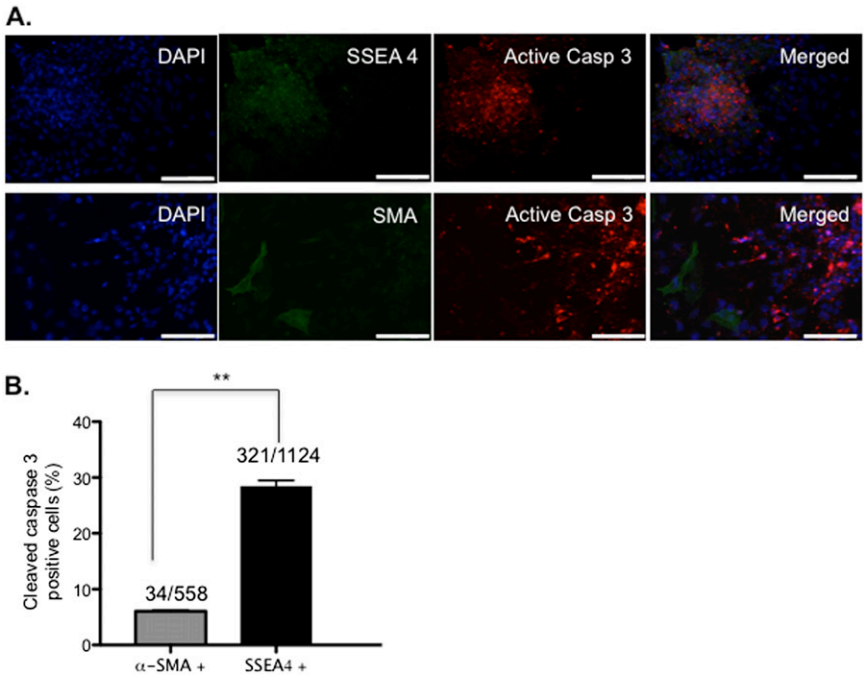

Fig. S5. (*A*) hiPSCs and smooth muscle cells derived from hiPSCs (SMC3) was mixed to 1:1 and were treated with 50 μM of QC for 24 h, followed by immunostaining analysis with SSEA-4 (green) and active caspase-3 (red) (*Upper*) or SMA (green) and active caspase-3 (red) (*Lower*). (Scale bars, 100 μm.) (*B*) Percentage of active caspase-3–positive population from either SMA-positive population or SSEA-3–positive population was determined by counting more than 500–800 cells and was graphically presented. $^{**}P < 0.01$.

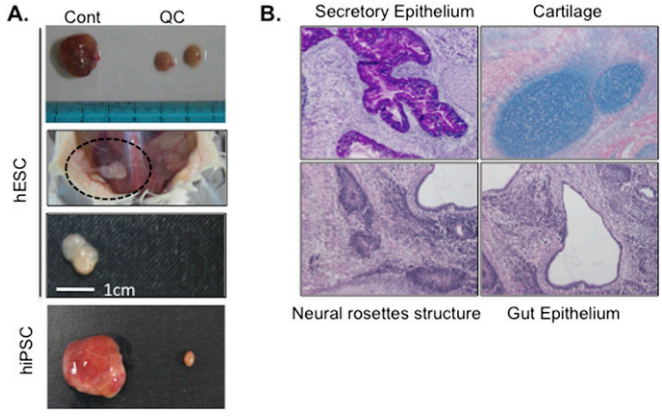

C.

Cell type	Injected Area	Cont	QC
hESCs	testis	3/3	0/3
	dorsum	1/1	0/1
Mixed hESCs	testis	1/1	0/1
hiPSCs	testis	1/1	0/1
Total		6/6	0/6

Fig. S6. (*A*) Representative images of teratomas formed by hESC and hiPSC in the presence or absence of a 50 μM QC pretreatment. (*B*) Teratomas sections generated by hESCs are shown stained with H&E, Masson's trichrome, and Alcian Blue. Teratomas produced cells indicative of gut epithelium, cartilage, secretory epithelium, and neural rosette structures. (*C*) Summary of teratoma formation with or without QC under three different conditions.

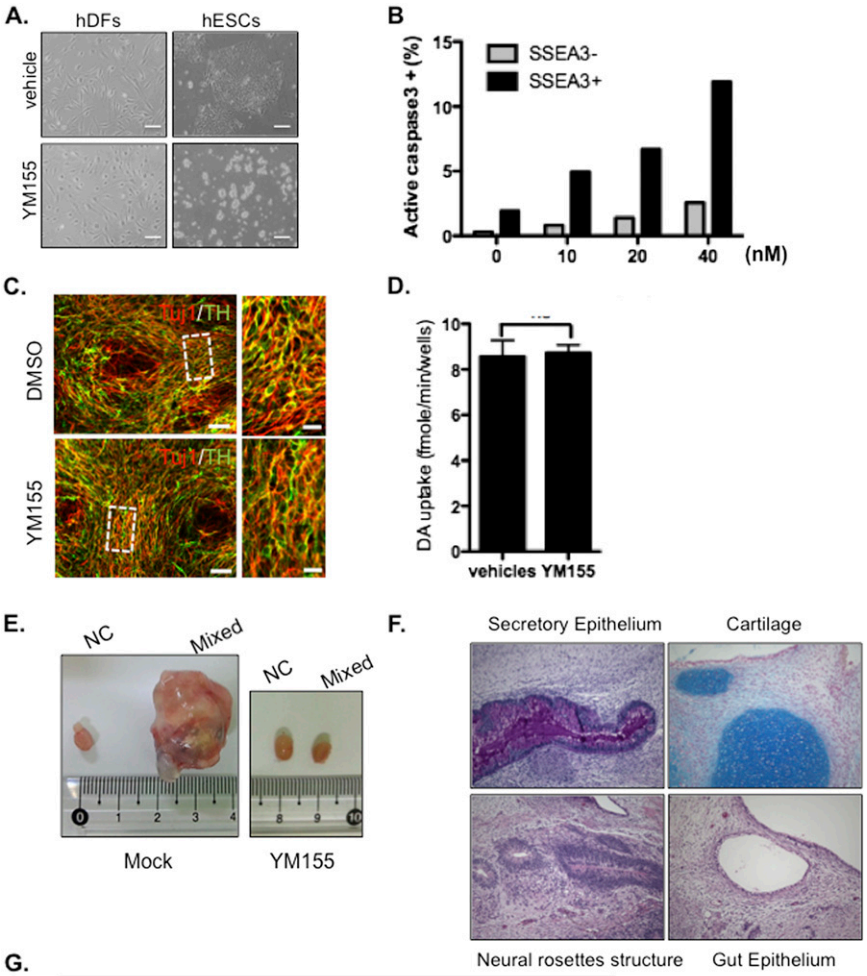

G.

Cell type	Injected Area	Cont	YM155
hESCs	testis	1/1	0/1
hiPSCs+SMCs	testis	1/1	0/1
Total		2/2	0/2

Fig. S7. (*A*) Light microscopic images of undifferentiated hESCs and fully differentiated human dermal fibroblast (hDF) treated with or without 10 nM of YM155. (Scale bars, 200 μm.) (*B*) Caspase-3 activity of hESCs and hDFs in response to treatment with the indicated dose of YM155 was determined using a caspase-3 activity assay. (*C*) Dopaminergic neuronal cells derived from hESCs were treated with 10 nM of YM155 or vehicle for 24 h and then subjected to dual immunostaining with Tuj (red) and TH (green) (*Left*). (*D*) Dopamine uptake of dopaminergic neuronal cells treated with 10 nM of YM155 or vehicle (DMSO) for 24 h was determined by measuring incorporation of [^{3}H]-labeled dopamine using liquid scintillation counting. ns, not significant. (*E*) A 1:1 mixture of hiPSCs and SMCs was injected into mouse testes. Representative images of teratomas formed in mouse testes injected with hESCs without (mock) or with 10 nM YM155 pretreatment (YM155). NC, no cells injected. (*F*) Teratomas sections generated by hESCs are shown stained with H&E, Masson's trichrome, and Alcian Blue. Teratomas produced cells indicative of gut epithelium, cartilage, secretory epithelium, and neural rosette structures. (*G*) Summary of teratoma formation with or without YM155 under three different conditions.

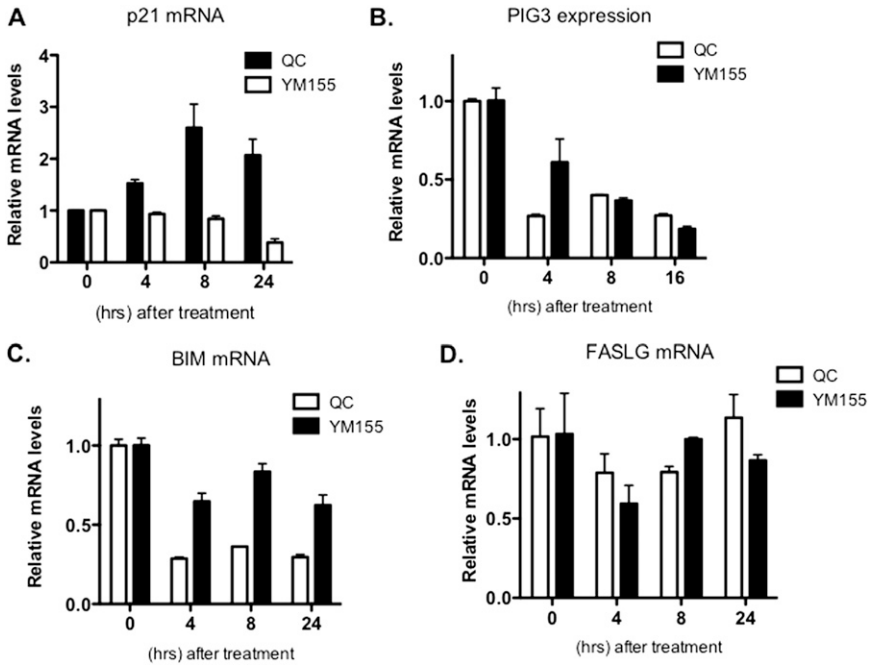

Fig. S8. hESCs were treated with 50 μM of QC or 10 nM of YM155 and were harvested at indicated times. p21CIP1 (*A*), p53 inducible gene 3 (*PIG3*) (*B*), Bcl2-interacting mediator of cell death (*BIM*) (*C*), and Fas-ligand (*FASLG*) (*D*) mRNA expression level was determined by real-time PCR analysis.

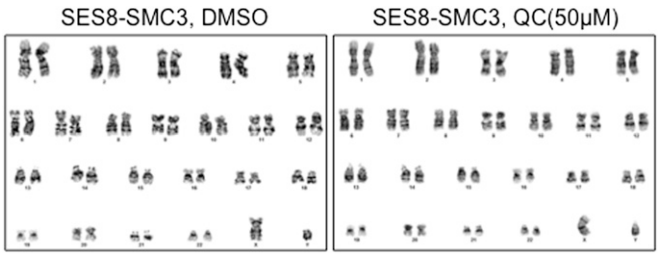

Fig. S9. Smooth muscle cells derived from hiPSCs (SMC3) were treated with 50 μM of QC for 24 h and were subjected to karyotyping analysis. Normal karyotyping (44+XY) after QC treatment.

Table S1. Pro- or antiapoptotic genes in hESCs

Gene	Description	Undif	Diff	Undff/Diff
Proapoptotic genes				
PYCARD	PYD and CARD domain containing	0.6311	0.002	401.43
DAPK1	Death-associated protein kinase 1	0.4106	0.002	261.20
CASP3	Caspase 3, apoptosis-related cysteine peptidase	0.2844	0.002	180.89
APAF1	Apoptotic peptidase activating factor	0.1412	0.002	89.82
TP53BP2	Tumor protein p53 binding protein, 2	0.1171	0.002	74.49
HRK	Harakiri, BCL2 interacting protein	0.0762	0.002	48.47
BCL2L11	BCL2-like 11 (apoptosis facilitator)	0.0731	0.002	46.49
BNIP1	BCL2/adenovirus E1B 19kDa interacting protein 1	0.0663	0.002	42.19
CRADD	CASP2 and RIPK1 domain containing adaptor with death domain	0.0598	0.002	38.03
CD70	CD70 molecules	0.0528	0.002	33.57
CD40	CD40 molecules	0.0420	0.002	26.70
CD27	CD27 molecules	0.0103	0.002	6.54
CASP2	Caspase 2, apoptosis-related cysteine peptidase	0.0978	0.019	5.24
CASP10	Caspase 10, apoptosis-related cysteine peptidase	0.0068	0.002	4.34
HPRT1	Hypoxanthinephosphoribosyltransferase 1 (Lesch-Nyhan syndrome)	1.0252	0.279	3.68
CIDEB	Cell death-inducing DFFA-like effector b	0.0650	0.023	2.846
CARD8	Caspase recruitment domain family, member 8	0.0044	0.002	2.77
TP73	Tumor protein p73	0.0043	0.002	2.71
TRAF2	TNF receptor-associated factor 2	0.1578	0.062	2.57
TNFRSF25	Tumor necrosis factor receptor superfamily, member 25	0.0171	0.007	2.55
TP53	Tumor protein p53 (Li-Fraumeni syndrome)	1.1064	0.479	2.31
CASP9	Caspase 9, apoptosis-related cysteine peptidase	0.2111	0.097	2.17
Antiapoptotic genes				
BCL10	B-cell CLL/lymphoma 10	0.0016	0.223	141.93
BCL2L2	BCL2-like 2	0.0016	0.068	43.38
BRAF	V-raf murine sarcoma viral oncogene homolog B1	0.0042	0.039	9.38
BAG1	BCL2-associated athanogene	0.0016	0.010	6.32
DFFA	DNA fragmentation factor, 45kDa, alpha polypeptide	0.2787	1.533	5.50
BAG4	BCL2-associated athanogene 4	0.0500	0.185	3.70
MCL1	Myeloid cell leukemia sequence 1 (BCL2-related)	0.3384	0.856	2.53
BFAR	Bifunctional apoptosis regulator	0.1365	0.318	2.33
BCL2	B-cell CLL/lymphoma 2	0.0037	0.008	2.07
BIRC6	Baculoviral IAP repeat-containing 6	0.0182	0.038	2.07

Table S2. List of cells in a database library

ESC lines	Adult stem cells	Normal cells
hESCs (H9)	T Lymphocyte (CD3- CD4+ CD8+) of peripheral blood	Extravillous trophoblast cell line HTR-8_SVneo
Embryoid body cell (H9)	pre-T Lymphocyte of thymus(DN3)	Extravillous trophoblast cell line SGHPL-5
Embryonic blast cell (H9)	T Lymphocyte (CD3+ CD4+ CD8+) of peripheral blood	Pharyngeal epithelial cancer cell line Detroit 562
hESCs (ES4)	pro-T Lymphocyte of thymus(DN1+DN2)	Kidney epithelial cell line HEK-293
hESCs (ES2)	Immature single positive T lymphocyte	Breast epithelial cell line HMEC
hESCs (HUES8)	T Lymphocyte (CD4+) of peripheral blood	Neonatal melanocyte cell line HEM-N
hESCs (HD129)	T Lymphocyte (CD8+) of peripheral blood	Melanocyte cell line HEM-LP
hESCs (HS181)	Erythroblast of peripheral blood	Melanocyte cell line Hermes 2B
hESCs (H7)	Myeloblast of bone marrow	Melanocyte cell line Hermes 1
hESCs (H14A)	Monoblast of peripheral blood	Embryonic skin fibroblast D551 cell line
hESCs (H13B)	Neutrophil of peripheral blood	Skin keratinocyte HaCaT cell line
hESCs (HD90)	Megakaryoblast of peripheral blood	Lung fibroblast cell line WI-38
hESCs (H14)	Monocyte of peripheral blood	Fibroblast of skin cell line GM-5659
hESCs (HS235)	Granulocyte-macrophage progenitor cell of bone marrow	Umbilical vein cell line HUVEC
hESCs (HD83)	Common myeloid progenitor cell of bone marrow	Neonatal foreskin keratinocyte NHEK cell line
hESCs (H9)	Megakaryocyte-erythrocyte progenitor cell of bone marrow	Testis fibroblast cell line Hs 1.Tes
hESCs (H13)	Hematopoietic stem cell of bone marrow	
hESCs (Cythera)	Eosinophil of peripheral blood	
hESCs (HUES6)	Basophil of peripheral blood	
hESCs (VUB01)	hESCs (H9)	
hESCs (BG01)	Embryoid body cell (H9)	
hESCs (CSES4)	Embryonic blast cell (H9)	
hESCs (H1)	Keratinocyte of foreskin	
hESCs (T3)	Transit-amplifying cell of skin	
hESCs (SA01)	Keratinocyte stem cell	
hESCs (WIBR2)	Tubular progenitor cell of kidney	
hESCs (WIBR1)	Glomerular progenitor cell of kidney	
hESCs (WIBR3)	Ovarian surface epithelial cell	
	Adipose stem cell	